

# Numerical Simulation of the methane air premixed flames and syngas air premixed flames inside a Micro Combustor with Different Inlet Wall Condition

Vijendra Masatkar, Suresh Kumar Badholiya

Bhopal Institute of Technology & Science, Bangrasia, Bhopal, Madhya Pradesh, India

## ABSTRACT

For methane-air mixture the flame structure of premixed CH<sub>4</sub>-air in a small tube with a parabolic and constant velocity profiles at inlet for various equivalence ratios is numerically investigated. The equivalence ratio is a key and dominating parameter that affects the combustion characteristics and hence the flame temperature. The highest flame temperature is obtained if the equivalence ratio is set at 0.9. The combustor geometry is an important factor which affects the zone of maximum temperature in combustor. In syn gas CO consumption rises with increase in combustor temperature while in methane CO concentration is maximum around outer envelope of flame it rises up to a certain temperature and decreases with further increase in temperature. In syn gas and methane carbon dioxide concentration decreases with increase in velocity because of incomplete combustion. For stoichiometric air-fuel ratios with same operating conditions syn gas emission of carbon mono oxide and carbon dioxide is more than methane-air mixture

**Keywords:** Velocity, Flame Temperature, Equivalence Ratio, Premixed Flames, Combustor Efficiency, Air Fuel Ration

## I. INTRODUCTION

Ever increasing demand of energy has initiated a revolutionary development in the field of MEMS devices like the concept of micro heat engine. The other devices based on the similar concept are micro gas turbine, micro thermoelectric devices, and micro thermo photovoltaic system. Micro-combustors are an essential and crucial component of such devices in which fuel and air mixture is allowed to burn. Use of micro combustors may be seen as convergence towards the approach of portable energy devices, which are using hydrocarbon as a main fuel and the traditional combustors. The micro-combustors are effectively used devices but also have certain issues which needed to be resolved before being allowed to use for domestic purposes. Owing to reduced size of the micro-combustors; length ranging from several millimeters down to less than a millimeter; combustion becomes extremely difficult under conditions of excessive heat loss from flame to combustor wall, radical destruction at gas-wall interface and low residence time rendering the system efficiency relatively low. Despite all challenges and difficulties ahead, the field of MEMS

devices is still growing and it is the most developing field in combustion. For hydrocarbon the quenching diameter is sufficient to stabilize the flame inside irrespective of other fuels having insufficient quenching length or diameter. By some previous experimental studies which demonstrated few interesting properties of hydrocarbon like CH<sub>4</sub> and O<sub>2</sub> having self sustained flames at 0.5 mm, which gives the luxury and freedom of using them in micro combustors. Unlike the experimental studies, numerical studies are able to yield the detailed information of compact zone. Flame temperature is one of the most dominating and key factor to analyze the process of combustion as the highest values of flame temperature can decide the material of micro combustor. The materials used generally are Aluminum oxide (alumina) and SiC with addition of some semi conductors. In this study effect of equivalence ratio, inlet velocity conditions on flame temperature will be investigated.

### 1.3 Emission norms:

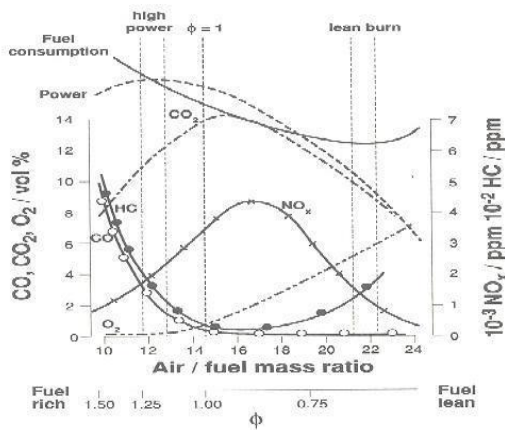


**Figure 1.1** Emission of pollutants in premixed combustion.

#### 1.3.1 Carbon Dioxide Emissions:

Since the start of the industrial revolution in the early 18<sup>th</sup> century, the increase in number of factories has largely increased the carbon dioxide emissions released into the atmosphere. The effects of carbon dioxide emissions have been pollution, extreme weather conditions, and global climate change. The most major problem that the increase in carbon dioxide emissions has brought though is the greenhouse effect. This happens when carbon dioxide takes in heat from the sun and the gas is trapped near the earth's surface, which causes global warming. The abiotic factors that affect carbon dioxide emissions are deforestation, pollution, and sunlight. Deforestation increases carbon dioxide emissions by killing trees that take in carbon dioxide. Pollution from factories releases carbon dioxide into the atmosphere and the carbon dioxide is heated by the sun to cause the greenhouse effect. Organisms that are affected by carbon dioxide emissions and global warming are polar bears, penguins, trout, caribou, orangutan, and the arctic fox. Although the main organism affected by carbon dioxide emissions and global warming is the polar bear. The polar bear lives in the arctic archipelagos and often swims in the Arctic Ocean. In the arctic habitat the polar bear mainly eats seals. They are negatively affected because the global warming causes the ice to melt, and when the ice melts the polar bears lose their habitat, hunting grounds, and place to raise their young. This could lead to the polar bear becoming extinct.

#### 1.3.2 Carbon monoxide:

The present study focuses on the investigation of the formation of CO and unburned oxygenated and no oxygenated hydrocarbon emissions from HCCI engines fueled with neat ethanol and neat isooctane. This is achieved with the use of a multimode model, which describes the essential features of HCCI combustion, that is, heat and mass transfer within the combustion chamber, both of which are modeled using phenomenological sub models. These mechanisms affect the formation of the main HCCI engine pollutants, namely, unburned hydrocarbons and carbon monoxide. Combustion is simulated using chemical kinetics coupled to oxidation mechanisms for isooctane and ethanol. These mechanisms also describe the decomposition of the original fuel into intermediate hydrocarbons and carbon monoxide. A validation of the model for both fuels is given for various load cases. In the numerical investigation, the formation of CO is described for the corresponding experimental cases and the essential features of the transition from CO production due to bulk quenching and to CO production due to post combustion partial HC oxidation are shown. Additionally, the formation of HC emissions is described including both oxygenated and no oxygenated compounds. This distinction was found to be necessary since both fuels include oxygenated species in the exhaust gases, the relative amount of which depends on load conditions and then fuel used.

#### 1.3.3 NOx emission:

There are several routes to form NO<sub>x</sub> pollutants and these may be broadly catalogued as thermally-generated, flame-generated, or fuel-bound NO<sub>x</sub>. Different authors use different names to catalogue these mechanisms and there is still continuing research to understand the most prominent mechanisms at ultra-low NO<sub>x</sub> conditions. For example, in hydrogen fuelled systems, the prominence of H radicals may contribute to NO<sub>x</sub> in a manner that is different than in systems fuelled by natural gas. Thermal NO<sub>x</sub> is formed by oxidation of nitrogen in air and requires sufficient temperature and time to produce NO<sub>x</sub>. A rule of thumb is that below approximately 1700K, the residence time in typical gas turbine combustors is not long enough to produce significant thermal NO<sub>x</sub>. Where temperatures higher than 1700K cannot be avoided, it is necessary to

limit residence time to control NO<sub>x</sub> formation, which favours very short combustor designs. Thermal NO<sub>x</sub> production also increases with the square root of operating pressure, making it more difficult to reduce in higher-pressure aero derivative gas turbines. As the name implies, flame-generated NO<sub>x</sub> occurs in the flame front, created on the short time scale associated with primary combustion reactions.

#### 1.4 Fuel used:

The fuel which possesses these is all qualities is Methane-air and syngas which is well known in field of combustion. Vehicles fuelled by methane blends are a first step toward a methane economy. These methane (natural gas) blends have the potential for environmental improvement with immediate reduction in emissions. Hydrogen is a clean fuel with no carbon emissions; the combustion of methane and syngas produces CO, CO<sub>2</sub> amount of nitrogen oxides. Conversely, combustion products from fossil fuels, such as CO, CO<sub>2</sub>, nitrogen oxides, or other air pollutants, cause health and environmental problems. But due to lower density of gas the specific volume of storage tank would be larger one which imposed the design constraints on designers to make feasible such a vehicle, also the extreme flammability and rapid burning of hydrogen is also a problem which violates its safety standards to be used as a domestic fuel. Although Hydrogen will help reduce CO<sub>2</sub> emissions as soon as it can be produced in a clean way either from fossil fuels, in combination with processes involving CO<sub>2</sub> capture and storage technologies, or from renewable energy. Even if hydrogen is seen as a key future energy carrier, it has several drawbacks. First, new technologies for production, storage, and transportation will have to be developed in order that we may begin to consider using hydrogen as an everyday fuel. Second, the flammable range of hydrogen is very wide (4–75%), and will require several safety standards to be redefined. Mixtures of natural gas and hydrogen can be part of a transitional pathway toward a hydrogen economy. These blends will allow reductions in emissions during which science can continue to develop technologies. Hydrogen/carbon monoxide oxidation kinetics has been of great interest in combustion research over decades, as it forms an important building block of the hydrocarbon combustion chemistry. There has also been a recent

interest in syngas produced by gasification of coal or biomass that primarily contains H<sub>2</sub>, CO, CO<sub>2</sub>, and H<sub>2</sub>O, as an alternative fuel in stationary power generation applications. Synthetic gas (syngas) is considered as one of the most promising alternative fuels that will play an important role in the diversification of the energetic sources since it can be produced from the gasification of coal, whose reserves are abundant worldwide, and multiple solid feedstock's such as organic waste and biomass. There have been previous studies related to laminar flame speed measurements of premixed H<sub>2</sub>/CO mixtures. The mode of combustion and the efficiency is closely related with the pattern of flame generation of fuel. Like the wave length and color of light itself shows the efficiency of combustion and species involved in combustion process, for example the blue color flame shows the full and complete burning of carbon like LPG cooking gases which burns with blue age flame. That is why the scope of flame analysis becomes wider to get a clear picture of insider and silent part of thermo chemistry.

Flames can be defined as the domain or region where oxidation of fuel takes place rapidly. It is an envelope of burning gases which is an exothermic chemical reaction which either proceeds with light or without light. Flames have following parts on major classifications.

Broadly classified as

- Diffusion flames
- Premixed flame.

##### 1.4.1 Diffusion flames:

In this style of combustion, fuel and air are introduced in separate passages, and the flame is stabilized where the fuel and air streams mix. Combustion reactions are typically so fast that fuel and oxidant consumption is limited by transport to the reaction zone (i.e., diffusion), and the reaction proceeds locally at nearly stoichiometric conditions. The Lewis number (Le) describes the ratio of thermal transport to species transport from this reaction zone. Where  $Le = 1$ , the temperature in the reaction zone will equal the adiabatic flame temperature because thermal energy diffuses away as fast as the reactants are supplied. The fuel species in hydrocarbon combustion typically have fuel Lewis numbers ( $Le_{mix} / Le_{fuel}$ ) in the range of 0.9 to 1.2, meaning that diffusion flame combustors will have

flame temperatures near the adiabatic flame temperature. These temperatures are high enough to oxidize nitrogen in air, producing

appreciable NO<sub>x</sub> pollutants. Hydrogen itself has a fuel Lewis number as low as 0.4, making it even more difficult to reduce NO<sub>x</sub> because the peak laminar flame temperatures are higher than adiabatic due to differential diffusion effects. The effect of fuel Lewis number on flame temperature has been observed experimentally as well as with direct numerical simulations (DNS).

#### 1.4.2 Premixed flame:

While in premixed combustion, as the name implies, premixed combustion is accomplished by mixing the fuel and air upstream of the flame. The fuel-air ratio normalized by the stoichiometric value is known as the equivalence ratio  $\phi$ , and in many practical premixed turbine combustors, has a value of slightly more than 0.5. Thus, there is approximately  $\frac{1}{2}$  the fuel needed to burn all the air, or conversely twice as much air as needed to burn all the fuel. The excess air serves to dilute the combustion and keep the flame temperatures low enough to avoid thermal NO<sub>x</sub> formation. While the concept of premixed combustion is simple and effective at reducing NO<sub>x</sub>, it also has drawbacks. The combustor must operate in a very narrow range of equivalence ratio to avoid blowout at (typically)  $\phi < 0.5$ , and increasing NO<sub>x</sub> formation for  $\phi$  somewhat greater than 0.6. The combustor controls must include some form of staging, since the range of desired exit temperatures usually cannot be achieved with such a small range of  $\phi$ . For example, if four fuel injectors are used in a combustor, it is possible to reduce the heat input 50% keeping two injectors operating, but turning two off. The difficulty with this approach is that the air flow from inactive injectors can quench the boundary of the flame from operating injectors, raising CO emissions, but this can be addressed with good aerodynamic design.

Flames can also be classified on the basis of their velocities of propagation.

- i) Deflagration flame
- ii) Detonation flame

Deflagration flames propagate at subsonic speed while Detonation flames propagate at supersonic speed. On same basis of velocity and flame shape flames are categorized as

- i) Laminar flame
- ii) Turbulent flame.

When the flames are formed without eddy formation and distortion in regular manner and shape they are classified as laminar flames on other hand if flames are distorted, random and in eddy form it is called as turbulent flame. Laminar flames are phenomenon and more theoretical which is explained in this literature with experimental figures and proposed work. Laminar flame speed is often an input as it has a significant impact upon the size and static stability of the combustor. Moreover it serves as a good validation parameter for leading kinetic models used for detailed combustion simulations.

## II. Literature Review

**[Niket S. Kaisare][2002][1]** A review on micro combustion: Fundamentals, devices and applications. Micro combustion research has flourished over the past decade. Yet, most of the commercial potential of micro combustion is still to come. Aside from portable electronics, emerging drivers stem from the energy problem of declining fossil fuel reserves and their large environmental footprint upon combustion. The need to capitalize on underutilized energy sources and renewable further stimulate energy research in micro systems. In this review paper, technological drivers, applications, devices, and fabrication protocols of micro burners are presented. Then, a review of homogeneous, catalytic, homogeneous-heterogeneous and heat recirculation micro burners is given. Results are presented that interpret literature findings. An outlook of micro combustion research is finally outlined.

**Natrajan and Jai Prakash [2008][2]** Experimentation and numerical investigation of laminar flame speeds of hydrogen, carbon monoxide, oxygen and nitrogen mixture (May 2008). The primary objective of this paper is to measure the laminar flame speeds and strain sensitivities of practical syngas fuel mixtures at realistic gas turbine conditions. To accomplish this goal two

flame speed measurement techniques have been developed to facilitate flame speed measurement for lean syngas fuel mixtures at elevated pressure but you did not answered and preheat temperature.

**[J. Natarajan, T. Lieuwen and J. Seitzman[2003].** Experimental and Numerical Investigation of Strained Laminar Flame Speeds for  $H_2/O_2/N_2$  Mixtures at Elevated Temperature. ( J. Natarajan, T. Lieuwen and J. Seitzman). Laminar flame speeds and strain sensitivities of mixtures of  $H_2$  and air, or air highly diluted with  $N_2$  ( $O_2:N_2$  1:9) have been measured for a range of equivalence ratios at high preheat conditions ( $\sim 700K$ ) using a nozzle generated, 1-

D, laminar, wall stagnation flame.

**M.R RAVI [2008] [3]** .Investigation of nitrogen dilution effects on the laminar burning velocity and flame stability of syngas fuel at atmospheric .The objective of this investigation was to study the effect of dilution with nitrogen on the laminar burning velocity and flame stability of syngas fuel (50%  $H_2$ –50% CO by volume)–air (21%  $O_2$ –79%  $N_2$  by volume) mixtures. The syngas fuel composition considered in this work comprised  $x\%$   $N_2$  by volume and  $(100 - x)\%$  an equimolar mixture of CO and  $H_2$ . The proportion  $x$  (i.e.,  $\%N_2$ ) was varied from 0 to 60% while the  $H_2/CO$  ratio was always kept as unity. Spherically expanding flames were generated by centrally igniting homogeneous fuel–air gas mixtures in a 40-L cylindrical combustion chamber fitted with optical windows. Shadow graphy technique with a high-speed imaging camera was used to record the propagating spherical flames. Unstretched burning velocity was calculated following the Karlovitz theory for weakly stretched flames.

**Anjan roy and M.R Ravi[] [ 5]** Effects of dilution with carbon dioxide on the laminar burning velocity and flame stability of  $H_2$  –CO mixtures at atmospheric condition. (Combustion and Flame) 482–492 by The objective of this investigation was to study the effect of dilution with  $CO_2$  on the laminar burning velocity and flame stability of syngas fuel (50%  $H_2$ –50% CO by volume). Constant pressure spherically expanding flames generated in a 40 l chamber were used for determining unscratched burning velocity. Experimental and numerical studies were carried out at

0.1 MPa,  $302 \pm 3$  K and  $\phi = 0.6 - 3.0$  using fuel-diluents and mixture-diluents approaches. For  $H_2$ –  $CO$ – $CO_2$ – $O_2$ – $N_2$  mixtures, the peak burning velocity shifts from  $\phi = 2.0$  for 0%  $CO_2$  in fuel to  $\phi = 1.6$  for 30%  $CO_2$  in fuel. For  $H_2$ – $CO$ – $O_2$ – $CO_2$  mixtures, the peak burning velocity occurred at  $\phi = 1.0$  unaffected by proportion of  $CO_2$  in the mixture.

**[Erjiang Hu, et. Al][6]** Experimental and numerical study on laminar burning characteristics of premixed methane–hydrogen–air flames

**[Zuohua Huang\*, Jiajia He, Chun Jin, Jianjun Zheng[2009][7]** An experimental and numerical study on laminar burning characteristics of the premixed Methane–hydrogen, air flames was conducted at room temperature and atmospheric pressure. The unscratched laminar burning velocity and the Markstein length were obtained over a wide range of equivalence ratios and hydrogen fractions. Moreover, for further understanding of the effect of hydrogen addition on the laminar burning velocity, the sensitivity analysis and flame structure were performed. The results show that the un-stretched laminar burning velocity is increased, and the peak value of the un-stretched laminar burning velocity shifts to the richer mixture side with the increase of hydrogen fraction.

**(Erjiang Hu, Zuohua Huang\*, Jiajia He, Haiyan Miao[8]** Experimental and numerical study on laminar burning velocities and flame instabilities of hydrogen–air mixtures at elevated pressures and temperatures Experimental and numerical study on hydrogen–air flames at elevated pressures and temperatures was conducted. Meanwhile, the calculation is extended to initial pressure and temperature up to 8.0 MPa and 950 K, respectively. Laminar burning velocities and Markstein lengths were obtained at the elevated pressures and temperatures. Sensitivity analysis and flame structure were also analyzed.

**Erjiang Hu, et. al. [2009] [9]** Numerical study on laminar burning velocity and NO formation of premixed methane–hydrogen–air flames .Numerical study on laminar burning velocity and NO formation of the premixed methane–hydrogen–air flames was conducted at room temperature and atmospheric pressure. The unscratched laminar burning velocity,

adiabatic flame temperature, and radical mole fractions of H, OH and NO are obtained at various equivalence ratios and hydrogen fractions.

**(Jeong Soo Kim a, Jeong Park a,\* , Dae Seok Bae a, Tran Manh Vu a, Ji Soo Ha b, Tae Kwon Kim[10]**A study on methane–air premixed flames interacting with syngas–air premixed flames .Numerical study on the interaction between methane–air and syngas–air premixed flames is conducted according to equivalence ratio and global strain rate in detailed chemistry. This study targets at understanding of an interacting combustion system as an alternative retrofit concept where one can modify the existing facilities minimally in industrial and power plant burners in order to reduce the emission of carbon dioxide.

**(Swarup Y. Jejurkar, D.P. Mishra[11].**Flame stability studies in a hydrogen air premixed flame Annular micro combustor Flame stability in an annular heat re-circulating micro combustor burning stoichiometric hydrogen air mixture was explored by means of a rigorous thermal analysis. The analysis is based on computational fluid dynamics model of reacting fluid flow accounting for interactions in flow, species, and conjugate thermal field in fluid and solid. Consideration of thermal diffusion effects in the model was necessary for realistic predictions in all the cases.

**Min Chul Lee,Seok Bin Seo, Jisu Yoon, Minki Kim, Youngbin Yoon[12]** Experimental study on the effect of N<sub>2</sub>, CO<sub>2</sub>, and steam dilution on the combustion performance of H<sub>2</sub> and CO synthetic gas in an industrial gas turbine. Combustion performance tests of syngas regarding the DR of N<sub>2</sub>, CO<sub>2</sub>, and steam at atmospheric pressure were successfully performed. From the results, the following conclusions are obtained.

**Sabre Bougrine, Ste´phane Richard , Andre´ Nicolle , Denis Veynante).[14]**This paper presents a numerical approach to evaluate premixed flame properties of CH<sub>4</sub>eH<sub>2</sub>-diluent mixtures by using complex chemistry. The proposed method is based on a priori simulations of 1D premixed flames to generate a wide chemical database. A benchmark of several available kinetic schemes of the literature was realized in order to evaluate and to choose the

more adapted kinetic mechanism to generate the database. y

**(Min Chul Lee,Seok Bin Seo , Jisu Yoon , Minki Kim , Youngbin Yoon)[15]** This result can be used for controlling, adjusting, and predicting the NO<sub>x</sub> emission of an IGCC plant that uses fuel dilution technology for NO<sub>x</sub> reduction

**(Erjiang Hu, Zuohua Huang[16].**Numerical study on laminar burning velocity and NO formation of premixed methane–hydrogen–air flames. Numerical study on laminar burning velocity and NO formation of the premixed methane hydrogen–air flames was conducted at room temperature and atmospheric pressure.

**A. Frassoldati, T. Faravelli, E. Ranzi.[17]** A wide range modeling study of NO<sub>x</sub> formation and nitrogen chemistry in hydrogen combustion .The chemistry of nitrogen species and the formation of NO<sub>x</sub> in hydrogen combustion are analyzed here on the basis of a large set of experimental measurements. The detailed kinetic scheme of H<sub>2</sub>/O<sub>2</sub> combustion was updated and upgraded using new kinetic and thermodynamic measurements, and was validated over a wide range of temperatures, pressures and equivalence ratios.

**B.C. Connelly, M.B. Long.M.D S mooke [18]** .Computational and experimental investigation of the interaction of soot and NO in co flow diffusion flames. A combined computational and experimental investigation that examines the relationship of soot formation and NO in co flow ethylene air diffusion flames is presented. While both NO and soot formation is often studied independently, there is a need to understand their coupled relationship as a function of system parameters such as fuel type, temperature and pressure.

### III. Mathematical Formulation

#### 3.1 Combustion modeling

##### 3.1.1 Introduction to Modeling Species Transport and Reacting Flows

FLUENT provides several models for chemical species transport and chemical reactions. This chapter provides an overview of the species transport and reaction models available in FLUENT.

### 3.1.2 Approaches to Reaction Modeling

FLUENT provides five approaches to modeling gas phase reacting flows:

1. Generalized finite-rate model.

This approach is based on the solution of transport equations for species mass fractions. The reaction rates that appear as source terms in the species transport equations are computed from Arrhenius rate expressions. You can use chemical kinetic mechanisms from the FLUENT database, create one yourself, or import a mechanism in Chemkin format. For turbulent flows, turbulence-chemistry interaction can be ignored using the Laminar Finite-Rate model, or modeled with the Eddy Dissipation or EDC models. The Generalized Finite-Rate Model is suitable for a wide range of applications including premixed, partially premixed, non-premixed turbulent combustion, and ignition delay in diesel engines. FLUENT can model the mixing and transport of chemical species by solving conservation equations describing convection, dilution, and reaction sources for each component species. Multiple simultaneous chemical reactions can be modeled, with reactions occurring in the bulk phase (volumetric reactions) and/or on wall or particle surfaces, and in the porous region. Species transport modeling capabilities, both with and without reactions.

#### 3.1.2.2 Non-Premixed Combustion model:

In non-premixed combustion, fuel and oxidizer enter the reaction zone in distinct streams. This is in contrast to premixed systems, in which reactants are mixed at the molecular level before burning. Examples of non-premixed combustion include pulverized coal furnaces, diesel internal-combustion engines and pool fires. Under certain assumptions, the thermo chemistry can be reduced to a single parameter: the mixture fraction. The mixture fraction, denoted by  $f$ , is the mass fraction that originated from the fuel stream. In other words, it is the local mass fraction of burnt and unburned fuel stream elements (C, H, etc.) in all the species (CO<sub>2</sub>, H<sub>2</sub>O, O<sub>2</sub>, etc.). The approach is elegant because atomic elements are conserved in

2. Non-premixed combustion model.
3. Premixed combustion model.
4. Partially premixed combustion model.
5. Composition PDF Transport model.

#### 3.1.2.1 Generalized Finite-Rate Model

Chemical reactions. In turn, the mixture fraction is a conserved scalar quantity, and therefore its governing transport equation does not have a source term. Combustion is simplified to a mixing problem, and the difficulties associated with closing non-linear mean reaction rates are avoided. Once mixed, the chemistry can be modeled as being in chemical equilibrium with the Equilibrium model, being near chemical equilibrium with the Steady Laminar Flame let model, or significantly departing from chemical equilibrium with the Unsteady Laminar Flame let model.

#### 3.1.2.3 Premixed Combustion Model

This model can be applied to turbulent combustion systems that are of the purely premixed type. In these problems perfectly mixed reactants and burned products are separated by a flame front. The "reaction progress variable" is solved to predict the position of this front. The influence of turbulence is accounted for by means of a turbulent flame speed.

In premixed combustion, fuel and oxidizer are mixed at the molecular level prior to ignition. Combustion occurs as a flame front propagating into the unburned reactants. Examples of premixed combustion include aspirated internal combustion engines, lean premixed gas turbine combustors, and gas-leak explosions. Premixed combustion is much more difficult to model than non-premixed combustion. The reason for this is that premixed combustion usually occurs as a thin, propagating flame that is stretched and contorted by turbulence. For subsonic flows, the overall rate of propagation of the flame is determined by both the laminar flame speed and the turbulent eddies. The laminar flame speed is determined by the rate that species and heat diffuse upstream into the reactants and burn. To capture the laminar flame speed, the internal flame structure would need to be resolved, as well as the detailed chemical kinetics and molecular dilution processes. Since practical laminar flame thicknesses are of the order of millimeters or smaller, resolution requirements are usually unaffordable. The effect of

turbulence is to wrinkle and stretch the propagating laminar flame sheet, increasing the sheet area and, in turn, the effective flame speed. The large turbulent eddies tend to wrinkle and corrugate the flame sheet, while the small turbulent eddies, if they are smaller than the laminar flame thickness, may penetrate the flame sheet and modify the laminar flame structure. In premixed flames, the fuel and oxidizer are intimately mixed before they enter the combustion device. Reaction then takes place in a combustion zone that separates unburned reactants and burnt combustion products. Partially premixed flames exhibit the properties of both premixed and diffusion flames. They occur when an additional oxidizer or fuel stream enters a premixed system, or when a diffusion flame becomes lifted of the burner so that some premixing takes place prior to combustion.

### Limitations:

- You must use the segregated solver. The premixed combustion model is not available with either of the coupled solvers.
- The premixed combustion model is valid only for turbulent, subsonic flows. These types of flames are called deflagrations. Explosions, also called detonations, where the combustible mixture is ignited by the heat behind a shock wave, can be modelled with the finite-rate model using the coupled solver. The premixed combustion model cannot be used in conjunction with the pollutant (i.e., soot and NO<sub>x</sub>) models. However, a perfectly premixed system can be modelled with the partially premixed model, which can be used with the pollutant models.
- You cannot use the premixed combustion model to simulate reacting discrete-phase particles, since these would result in a partially premixed system. Only inert particles can be used with the premixed combustion model.

In many industrial premixed systems, combustion takes place in a thin flame sheet. As the flame front moves, combustion of unburned reactants occurs, converting unburned premixed reactants to burnt products. The premixed combustion model thus considers the reacting flow field to be divided into regions of burnt and unburned species, separated by the flame sheet.

$$\left(\frac{\partial}{\partial t}\right) + \nabla \cdot (\rho \vec{\partial} c) = \nabla \cdot \left(\frac{\mu}{sc} \nabla c\right) + \rho_c \delta c$$

C = Mean reaction progress variable

S<sub>Ct</sub> = Turbulent Schmidt number

δ<sub>c</sub> = Reaction progress source term

the progress variable is defined as a normalized sum of product species .

$$c = \frac{\sum_{i=1}^n Y_i}{\sum_{i=1}^n Y_{i,e,q}}$$

Y<sub>i</sub> = mass fraction of products species i.

Y<sub>i,e,q</sub> = Equilibrium mass fraction of product species .

n = number of products.

Based on this definition, C=0 where the mixture is unburned and C=1 where the mixture is burnt.

### 3.2 NO<sub>x</sub> Formation:

NO<sub>x</sub> emission consists of mostly nitric oxide (NO), and to a lesser degree nitrogen dioxide (NO<sub>2</sub>) and nitrous oxide (N<sub>2</sub>O). NO<sub>x</sub> is a precursor for photochemical smog, contributes to acid rain, and causes ozone depletion. Thus, NO<sub>x</sub> is a pollutant. The **FLUENT** NO<sub>x</sub> model provides a tool to understand the sources of NO<sub>x</sub> production and to aid in the design of NO<sub>x</sub> control measures. The **FLUENT** NO<sub>x</sub> model provides the capability to model thermal, prompt, and fuel NO<sub>x</sub> formation as well as NO<sub>x</sub> consumption due to re-burning in combustion systems. . NO<sub>x</sub> reduction using reagent injection, such as selective non catalytic reduction (SNCR), can be modeled in **FLUENT** along with an N<sub>2</sub>O intermediate model which has also been incorporated. To predict NO<sub>x</sub> emissions, **FLUENT** solves a transport equation for nitric oxide (NO) concentration. When fuel NO<sub>x</sub> sources are present, **FLUENT** solves additional transport equations for intermediate species (HCN and/or NH<sub>3</sub>). When the N<sub>2</sub>O intermediate model is activated, an additional transport equation for N<sub>2</sub>O will be solved. The NO<sub>x</sub> transport equations are solved based on a given flow field and combustion solution. In other words, NO<sub>x</sub> is post processed from a combustion simulation. It is thus evident that an accurate combustion solution becomes a prerequisite of NO<sub>x</sub> prediction. For example, thermal NO<sub>x</sub> production doubles for every 90 K temperature increase when the flame temperature is about 2200 K. Great care must be exercised to provide accurate thermo physical data and boundary condition inputs for the combustion model. Appropriate turbulence, chemistry, radiation and other sub-models must be employed. To be realistic, one can only expect results to be as accurate as the input data and the selected physical models. Under most circumstances, NO<sub>x</sub>



variation trends can be accurately predicted but the NO<sub>x</sub> quantity itself cannot be pinpointed. Accurate prediction of NO<sub>x</sub> parametric trends can cut down on the number of laboratory tests, allow more design variations to be studied, shorten the design cycle, and reduce product development cost. That is truly the power of the **FLUENT** NO<sub>x</sub> model and, in fact, the power of CFD in general. The following represents the theoretical background of NO<sub>x</sub> formation and predictions about usage of solutions employed by solver.

### 3.2.1 Overview and Limitations.

- Governing Equations for NO<sub>x</sub> Transport.
- Thermal NO<sub>x</sub> Formation.
- Prompt NO<sub>x</sub> Formation.
- Fuel NO<sub>x</sub> Formation.
- NO<sub>x</sub> Formation by Re-burning.
- Formation in Turbulent Flows.
- Using the NO<sub>x</sub> Model.

#### Overview and Limitations:

NO<sub>x</sub> emission consists of mostly nitric oxide (NO). Less significant are nitrogen oxide (NO<sub>2</sub>) and nitrous oxide (N<sub>2</sub>O). NO<sub>x</sub> is a precursor for photochemical smog, contributes to acid rain, and causes ozone depletion. Thus, NO<sub>x</sub> is a pollutant. The **FLUENT** NO<sub>x</sub> model provides a tool to understand the sources of NO<sub>x</sub> production and to aid in the design of NO<sub>x</sub> control measures.

### 3.3 Nox Modeling In FLUENT:

The **FLUENT** NO<sub>x</sub> model provides the capability to model thermal, prompt, and fuel NO<sub>x</sub> formation as well as NO<sub>x</sub> consumption due to re-burning in combustion systems. It uses rate models developed at the Department of Fuel and Energy, The University of Leeds, England as well as from the open literature. To predict NO<sub>x</sub> emission, **FLUENT** solves a transport equation for nitric oxide (NO) concentration. With fuel NO<sub>x</sub> sources, **FLUENT** solves an additional transport equation for an intermediate species (HCN or NH<sub>3</sub>). The NO<sub>x</sub> transport equations are solved based on a given flow field and combustion solution. In other words, NO<sub>x</sub> is post processed from a combustion simulation. It is thus evident that an accurate combustion solution becomes a prerequisite of NO<sub>x</sub> prediction. For example, thermal NO<sub>x</sub> production doubles for every 90 K temperature increase when the

flame temperature is about 2200 K. Great care must be exercised to provide accurate thermo physical data and boundary condition inputs for the combustion model. Appropriate turbulence, chemistry, radiation and other sub-models must be applied. To be realistic, one can only expect results to be as accurate as the input data and the selected physical models. Under most circumstances, NO<sub>x</sub> variation trends can be accurately predicted but the NO<sub>x</sub> quantity itself cannot be pinpointed. Accurate prediction of NO<sub>x</sub> parametric trends can cut down on the number of laboratory tests development cost. That is truly the power of the **FLUENT** NO<sub>x</sub> model and, in fact, the power of CFD in general.

### 3.3.1 The Formation of NO<sub>x</sub> in Flames:

In laminar flames, and at the molecular level within turbulent flames, the formation of NO<sub>x</sub> can be attributed to four distinct chemical kinetic processes: thermal NO<sub>x</sub> formation, prompt NO<sub>x</sub> formation, fuel NO<sub>x</sub> formation, and re-burning. Thermal NO<sub>x</sub> is formed by the oxidation of atmospheric nitrogen present in the combustion air. Prompt NO<sub>x</sub> is produced by high-speed reactions at the flame front, and fuel NO<sub>x</sub> is produced by oxidation of nitrogen contained in the fuel. The re-burning mechanism reduces the total NO<sub>x</sub> formation by accounting for the reaction of NO with hydrocarbons. The **FLUENT** NO<sub>x</sub> model is able to simulate all four of these processes.

### 3.3.1 Restrictions on NO<sub>x</sub> Modeling:

1. You must use the segregated solver. The NO<sub>x</sub> models are not available with either of the coupled solvers
2. The NO<sub>x</sub> models cannot be used in conjunction with the premixed combustion model.

#### Governing Equations for NO<sub>x</sub> Transport:

**FLUENT** solves the mass transport equation for the NO species, taking into account convection, dilution, production and consumption of NO and related species. This approach is completely general, being derived from the fundamental principle of mass conservation. The effect of residence time in NO<sub>x</sub> mechanisms, a Lagrangian reference frame concept, is included through the convection terms in the governing equations written in the Eulerian reference frame. For thermal and only the NO species transport equation is

needed. Allow more design variations to be studied, shorten the design cycle, and reduce product

$$\frac{\partial}{\partial t}(\rho Y_{NO}) + \nabla(\rho \vec{\theta} Y_{NO}) = \nabla(\rho D Y_{NO}) + \delta_{NO} \quad (3.2.1)$$

$$\frac{\partial}{\partial t}(\rho Y_{HCN}) + \nabla(\rho \vec{\theta} Y_{HCN}) = \nabla(\rho D Y_{HCN}) + \delta_{HCN} \quad (3.2.2)$$

In mid 18th century, the French engineer Claude Navier and the Irish mathematician George Stokes equations. These equations have been derived based on the fundamental governing equations of fluid dynamics, called the continuity, the momentum and the energy equations, which represent the conservation laws of physics.

## IV. Results

### 4.1 Validation:

A reference case is always needed to compare and examine the most precise results. Here the reference is 2 mm diameter tubular combustor having 12 mm length with results derived in reference literature. In mixture of methane-air very low velocities are employed in order of 0.3 m/s to 1 m/s because higher velocities results in higher mass flow rate. As velocities increases it can be seen by contours that reaction zone of methane burning is also shifts towards downstream. Also implies that at lower velocities the highest temperature is visible on axis but as velocity increases the higher temperature zone is shifted towards the wall. This happens due to consumption of methane near the wall is more at higher velocities than that of lower velocities. After all the velocity has no significant influence on highest value of flame temperature.

#### 4.1.1 Effect of Inlet velocity:

The effects of inlet velocity of the methane-air mixture on the flame temperature along the axis of the combustor ( $r \leq 40$ ) are shown in below. The inlet of the micro-combustor is located at  $x \leq 0.03$  m and the outlet is located at  $x \leq 0.04$  m. From this figure, one can see that as the inlet velocity increases, the location of the peak value of the flame temperature at the axis of the combustor, i.e., the flame front is shifted downstream. The peak flame temperature increases with the inlet velocity first to a certain value for smaller inlet velocities and then, after the inlet velocity exceeds a certain critical value (e.g.  $\leq 0.8$  m/s), this peak temperature remains a constant and is independent of

the inlet velocity. These results show that as the velocity increases, the main reaction zone shifts downstream. With the existence of the wall temperature gradient, at relatively low inlet velocities (e.g.  $\leq 0.8$  m/s) the flame location is in front of the highest wall temperature zone. Due to the relatively weak convective heat transfer and the smaller temperature difference between the methane air mixture and the wall, the mixture is not fully preheated before combustion is completely actuated, and this will certainly lead to a relatively low flame temperature. As the inlet velocity increases, the main reaction zone shifts downstream. The convective heat transfer and the temperature difference between the methane air mixture and the wall are enlarged; the mixture is thus well preheated, so the flame temperature increases with the inlet velocity. However, as the velocity exceeds a certain value (e.g. 0.8 m/s), the flame front is shifted further to the downstream, the convection heat transfer coefficient and the temperature difference between

### 4.2 Computational details

The discretized model is a cylindrical micro combustors Fig 4.1 shows cross-sectional view of a two-dimensional micro-combustor in which methane and air are allowed to burn. The combustor may be considered as either a cylindrical tube ( $d = 1$  and 2 mm) or parallel plates maintained at the same distance apart as the tube diameter. The thickness of combustor wall is taken finite (0.2 mm) and length as 12 mm. The origin is fixed at centre line of the combustor inlet. X and Y co-ordinates show axial and radial variations respectively in micro combustor.

The flow is considered steady and axis-symmetric which renders the problem 2D symmetric. By certain design and computational assumptions the swirl component of velocity is taken as zero. The computations are performed only in half of the domain for the sake of economic usage of computational time. The following assumptions are also invoked to further simplify the problem.

#### 4.2.1 Computational domain and boundary conditions

The geometric size of the rectangular computational domain and the boundary conditions imposed for all simulations are shown in Fig. 4.7.1 The size of the whole computational domain is  $12D \times 2D$ , where D is

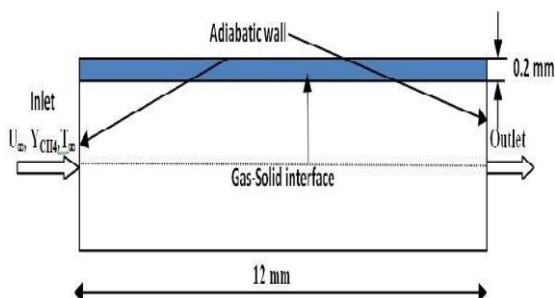
the diameter of cylinder. The upper and lower boundaries are located at a distance 7D from the centre of the cylinder; this ensures that these boundaries have no effect on the flow around the cylinder. The flow inlet is located 7D upstream from the centre of the cylinder, and the flow outlet is located 20D downstream from the centre of the cylinder. These distances are sufficient to eliminate the far field effects on the flow upstream and downstream of the cylinder.

Fig 4.1 shows cross-sectional view of a two-dimensional micro-combustor in which methane and air are allowed to burn. The combustor may be considered as either a cylindrical tube (d

= 1 and 2 mm) or parallel plates maintained at the same distance apart as the tube diameter. The thickness of combustor wall is taken finite (0.2 mm) and length as 12 mm. The origin is fixed at centre line of the combustor inlet. X and Y co-ordinates show axial and radial variations respectively in micro combustor. The flow is considered steady and axi-symmetric which renders the problem 2D symmetric. By certain design and computational assumptions the swirl component of velocity is taken as zero. The computations are performed only in half of the domain for the sake of economic usage of computational time. The following assumptions are also invoked to further simplify the problem:

- 1) No Dufour effects.
- 2) No gas radiation.
- 3) No work done by pressure and viscous forces.

With these assumptions, the equations of continuity, momentum, species and energy in the gas phase (for the cylindrical micro-combustor) can be written as follows:



**Figure 4.1 :** Computational domain and the imposed boundary conditions.

The boundary conditions used for the numerical simulations are as follows:

### Boundary Conditions:

The boundary conditions are given as follows:

#### Inlet:

At inlet ( $x = 0$ ):  $T_u = 300K$ ,  $u_0 = 0.3, 0.5, 0.8$  and  $1.0$  m/s.  $Y_{CH_4} = 0.05$ ,  $Y_{O_2}$  can be derived for a equivalence ratio of 0.9 and the air composition.

$$q_w = h_{conv} (T_{w\infty} - T_\infty) + \epsilon\sigma (T_{w\infty}^4 - T_\infty^4)$$

fluxes are considered zero, i.e. at  $r = 0$ ,  $\partial u/\partial r = 0$ ,  $\partial T/\partial r = 0$ ,  $\partial Y_i/\partial r = 0$ ,  $v = 0$ .

#### Gas-solid interface:

## V. Results and discussion

### 5.1 Validation:

A reference case is always needed to compare and examine the most precise results. Here the reference is 2 mm diameter tubular combustor having 12 mm length with results derived in reference literature. In mixture of methane-air very low velocities are employed in order of 0.3 m/s to 1 m/s because higher velocities results in higher mass flow rate. As velocities increases it can be seen by contours that reaction zone of methane burning is also shifts towards downstream. Also implies that at lower velocities the highest temperature is visible on axis but as velocity increases the higher temperature zone is shifted towards the wall. This happens due to consumption of methane near the wall is more at higher velocities than that of lower velocities. After all the velocity has no significant influence on highest value of flame temperature.

#### 4.1.1 Effect of Inlet velocity:

The effects of inlet velocity of the methane-air mixture on the flame temperature along the axis of the combustor ( $r=0$ ) are shown in below. The inlet of the micro-combustor is located at  $x=0.03$  m and the outlet is located at  $x=0.04$  m. From this figure, one can see that as the inlet velocity increases, the location of the peak value of the flame temperature at the axis of the combustor, i.e., the flame front is shifted downstream. The peak flame temperature increases with the inlet velocity first to a certain value for smaller inlet

velocities and then, after the inlet velocity exceeds a certain critical value (e.g.  $\approx 0.8$  m/s), this peak temperature remains a constant and is independent of the inlet velocity. These results show that as the velocity increases, the main reaction zone shifts downstream. With the existence of the wall temperature gradient, at relatively low inlet velocities (e.g.  $\approx 0.8$  m/s) the flame location is in front of the highest wall temperature zone. Due to the relatively weak convective heat transfer and the *smaller temperature difference between the methane air mixture and the wall, the mixture is not fully preheated* before combustion is completely actuated, and this will certainly lead to a relatively low flame temperature. As the wall and the methane-air mixture acquire their maximum values for the given thermal boundary conditions. The mixture is thus preheated to its highest possible temperature, and therefore the peak flame temperature reaches to its highest value for the given thermal conditions. After this, although the reaction zone shifts downstream further as the velocity increases, the peak flame temperature remains its highest value and is independent of the inlet velocity. These results also show that the heat transfer condition between the methane-air mixture and the wall may strongly influence the characteristics of combustion. The influence of the inlet velocity on the mass fraction of  $\text{CH}_4$  along the axis is shown below. For relatively low inlet velocities,  $\text{CH}_4$  is burned out within a very narrow zone. The reaction zone increases with the inlet velocity due to the intensified mass transfer along the axis which makes  $\text{CH}_4$  diffuse further downstream. It can be seen from figures, the axial velocity of the mixture increases sharply in the combustion zone. In the combustion zone, the huge amount of the heat produced by combustion is released in a very small distance and thus causes the sharp increase of the velocity in the region. Then after the combustion is finished and due to the strong heat transfer between the fluid and the wall, a lot of the heat is dissipated to the environment, the mixture is thus cooled down and therefore its velocity decreases along the flow

the inlet velocity increases, the main reaction zone shifts downstream. The convective heat transfer and the temperature difference between the methane air mixture and the wall are enlarged; the mixture is thus well preheated, so the flame temperature increases with the inlet velocity. However, as the velocity exceeds a certain value (e.g. 0.8 m/s), the flame front is shifted further to the downstream, the convection heat transfer coefficient and the temperature difference between direction. Since the tube or combustor is actually supposed to be infinite, there does not exist a blow-out velocity. The increase in the inlet velocity will push the combustion front downstream.

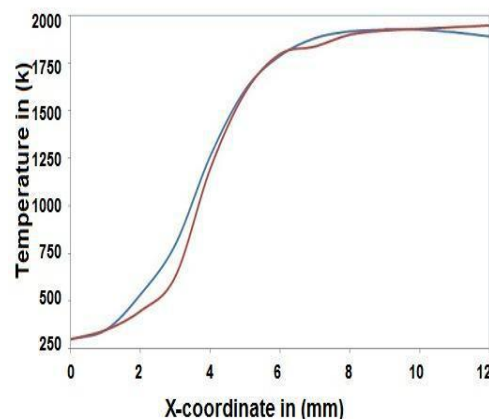


Fig. 5.1: Validation of maximum flame temperature at axis with velocity 0.8 m/s.

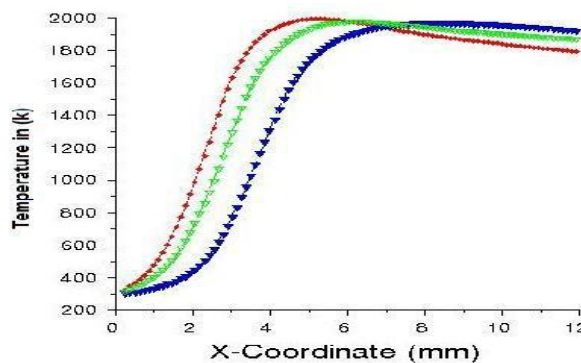


Fig. 5.2: Temperature contour of validated curve at **axis of combustor.**

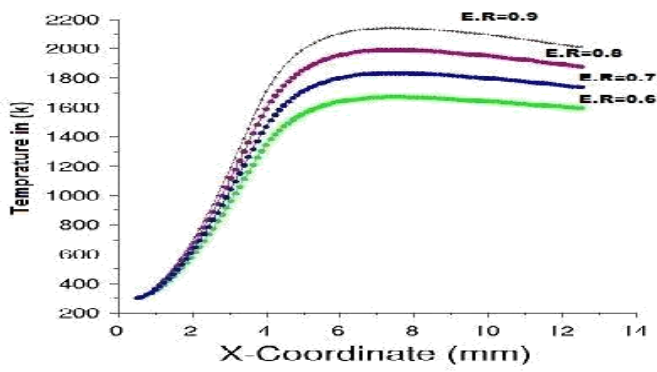


Fig. 5.3: Axial advancement of flame temperature with increase in velocity.

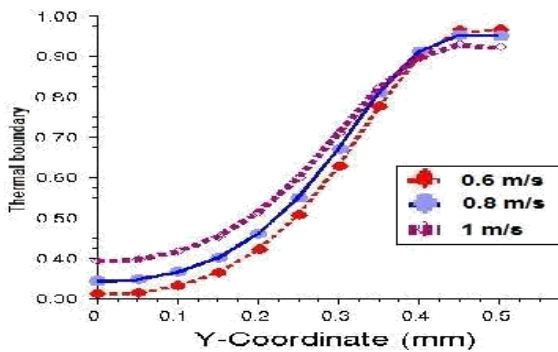


Fig. 5.4: Temperature contours at various velocities at axis of combustor

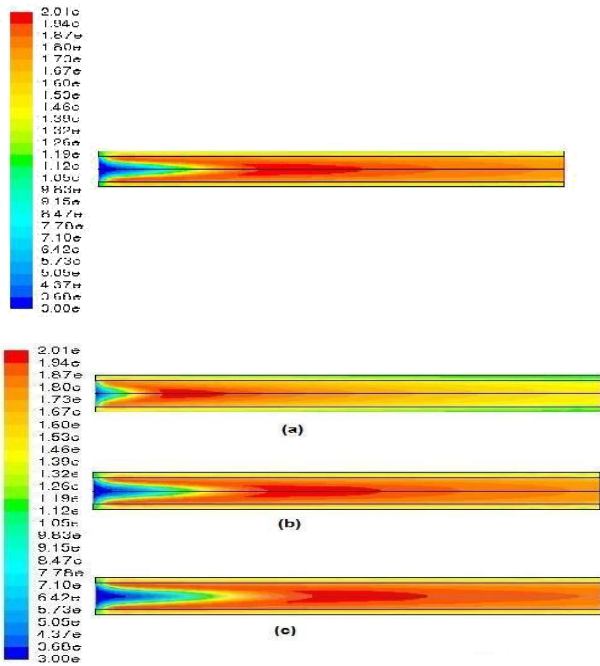


Fig. 5.5: Mass fraction of methane at various velocities at axis of combustor.

$$\text{Equivalence ratio } (\varphi) = \frac{\text{fuel air ratio}}{\text{stoichiometric fuel air ratio}}$$

### 5.1.2 Effect of equivalence ratio.

The equivalence ratio can be described as the ratio of fuel-air to the ratio stoichiometric fuel-air ratio. It is denoted by  $\varphi$

Equivalence ratio can be defined as follows

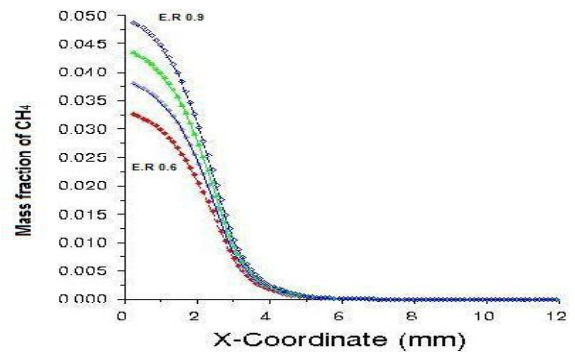


Fig. 5.6: Temperature rise at axis with various equivalence ratios.

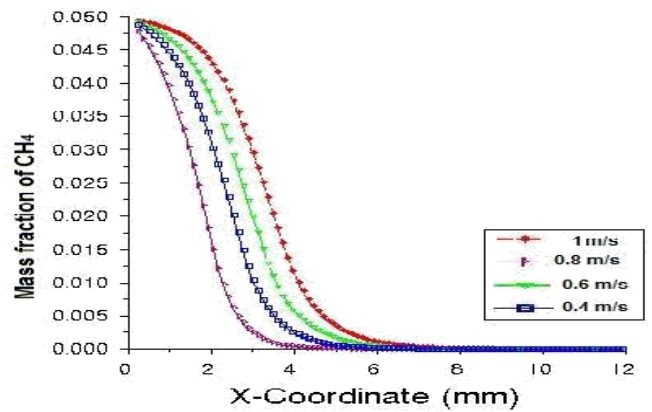


Fig. 5.7: methane mass fraction at axis with increase in equivalence ratio.

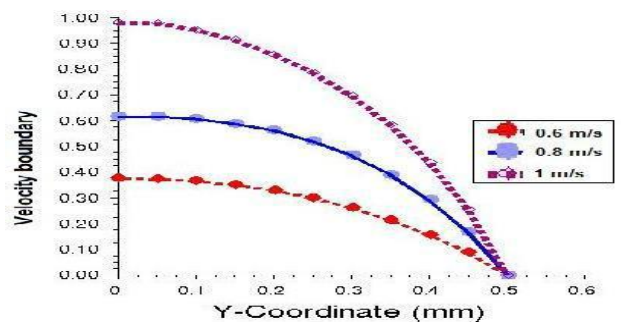
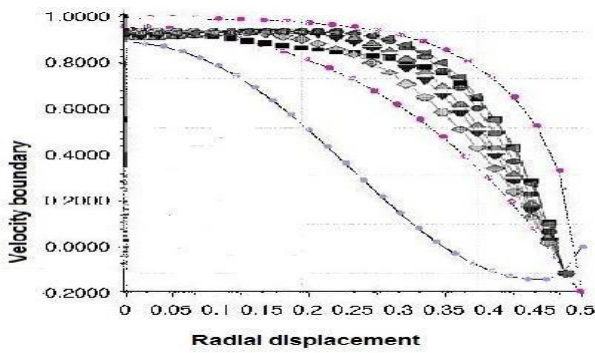
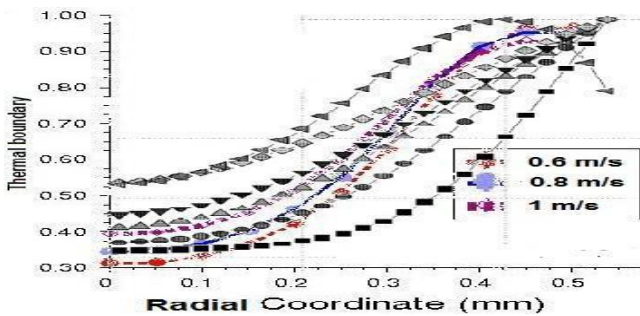


Fig. 5.8: radial velocity variation with increase in wall thickness



**Fig. 5.9: Radial temperature variation at inlet with different velocities.**



**Fig. 5.10: Validation of results of radial velocity.**

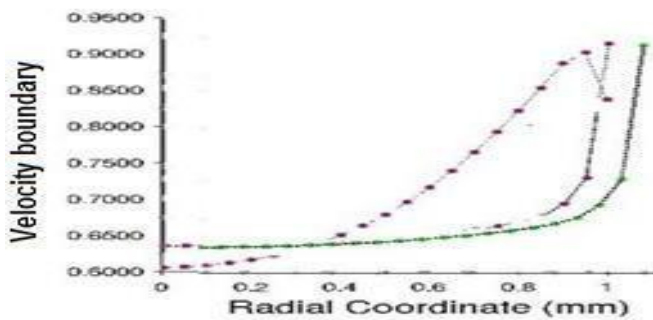


**Fig. 5.11: Validation of results of temperature rise at inlet.**

In 2mm combustor the velocity rise and temperature rise are not as sharp as like 1mm combustor due to larger radius. In 2mm combustor the radial convection is more due to larger passage is available as shown in **Fig. 5.12** and **5.13**. Here the heat transfer is more hence the drop in temperature is also more, which leads the temperature profile less steeper as compared to 1mm diameter. In 1mm diameter combustor the axial convection is more due to less space in radial direction.

**Fig. 5.12: Radial temperature variation at inlet for 2mm combustor.**

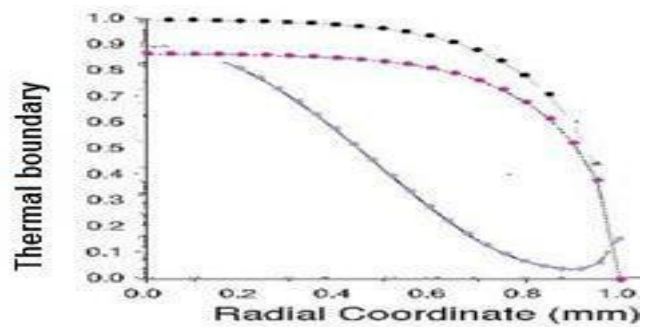


**Fig. 5.13: Radial velocity variation with increase in wall thickness.**

The **Fig 5.8 & 5.9** shows the variation in temperature and velocity profiles in radial direction for 1mm combustor, for both of combustors the velocity and temperature profiles are almost same in shape only. While **Fig.5.10** and **Fig. 5.11** are standard validation of temperature velocity with standard published literature

#### 5.1.4 Effect of geometry:

Combustor geometry is an important and considerable parameter under micro combustors. For comparison we have analyzed two combustors having different diameters like 1 mm and 2 mm. In 1 mm diameter for a given length of 12 mm the phenomenon of radial diffusion occurs more significantly than axial convection. This shows the temp contour extended and radial direction but while diameter is doubled the axial convection is dominating in 2mm diameter. The temperature contour of 1mm and 2 mm combustors are shown in following **Fig. 5.14**. Also for a given velocity 1mm diameter combustor can show higher temperatures for the flames. The length is also an important criterion in micro combustors because higher

lengths (20d to 25d) provide higher axial variation in temperatures and also higher convection length for wall and fluid interface Fig. 6 shows temperature contours of 1mm diameter combustor and 2mm diameter combustor. As (a) and (b) indicates the reaction zone is longer in 1mm diameter than 2 mm diameter combustor for same length. In 2mm diameter combustor the maximum temperature zone is seen near the walls but in 1 mm diameter it is seen at axis itself because double diameter increases the radial diffusion towards the walls. Also in large combustor the heat diffuses towards the wall and hence temperature is more governed by radial factor itself in small diameter combustor the dominating parameter is axial convection. Another main parameter is heat circulation on walls which is more in small combustor. For same equivalence ratio 1mm diameter combustor shows higher flame temperatures than larger combustors. analyze the influences of the combustor size on the characteristics of combustion, numerical simulations are performed for inlet velocity of 0.5 m/s and the equivalence ratio of 0.85 over a range of the combustor tube diameters.

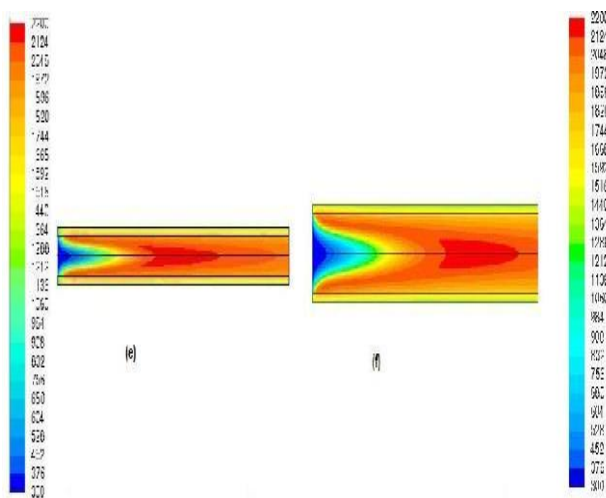


**Fig. 5.14: Temperature contours for 1mm and 2mm diameter combustor.**

### 5.1.5 Effect of wall conditions:

The wall temperature is a factor which decides the temperature distribution around the flame envelope. The intensity of maximum temperature spots can be controlled with the wall temperature itself. In small combustors the complex shape results in the intense heat losses by flames which affect efficiencies

directly. Here different wall conditions show the variation in flame temperature and stability at different temperatures. An axial temperature profile is setup through walls to investigate the effects of heated wall

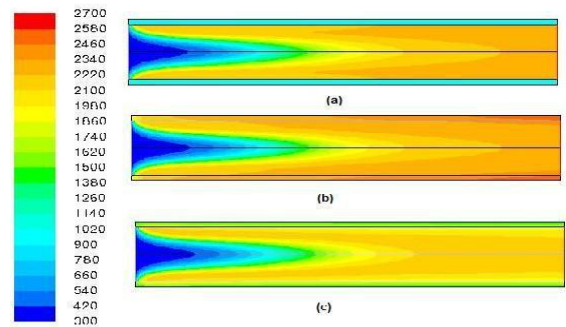


**Fig. 5.15: Temperature contours with different wall conditions.**

**Fig.5.15.** depicts contours of temperature for different wall conditions, viz., (a) the wall has an axial thermal gradient, in (b) walls are adiabatic with zero heat flux and in (c) the walls are having all possible modes of heat transfer. Consequences of temperature gradient can be easily predicted by **Fig. 5.15(a)** where the maximum temperature is distributed towards the wall. In case of insulated walls the flame temperature at axis is maximum around 2400 K and minimum for coupled wall conditions for methane flame.

## 5.2 Parametric study

### (a) Calculation of carbon dioxide and carbon monoxide:

#### 5.2.1 Effect of combustor diameter and formation of knife edge:

Combustor diameter plays an important role in stabilizing flame inside a combustor. Smaller diameter provides lesser space for radial convection as compared to the large diameter tube during combustion process. These effects of geometry lead flame to form a conical shape with sharp edge which is known as knife edge. A fuel with high flammability like syngas also forms knife edge in smaller combustors.

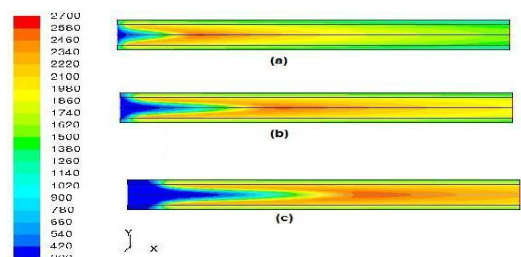


**Fig. 5.16: Knife edge formation in 1mm combustor with syn gas at various velocities.**

carbon mono oxide formation zone at axis . The inlet velocity has almost no significant effect on maximum temperature of flame, but strong effect on outlet emission norms.

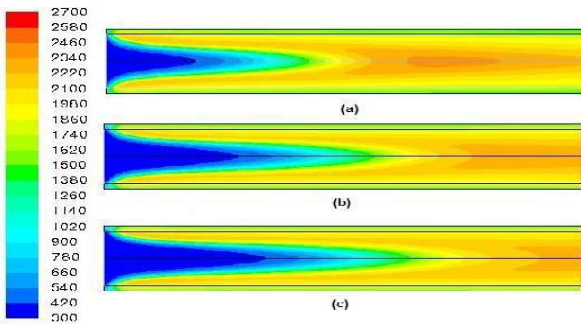


**Fig. 5.17: Temperature contour of 2mm combustor with syn gas at various velocities.**

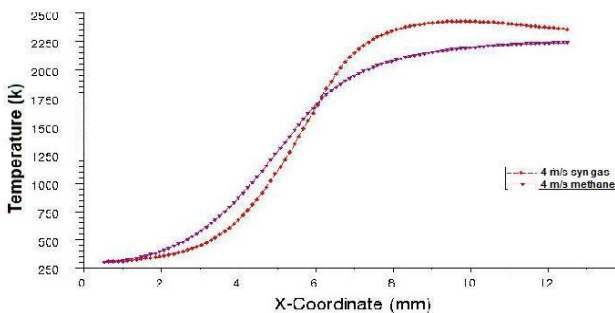


**Fig. 5.18: Comparison of maximum temperature between methane and syngas.**

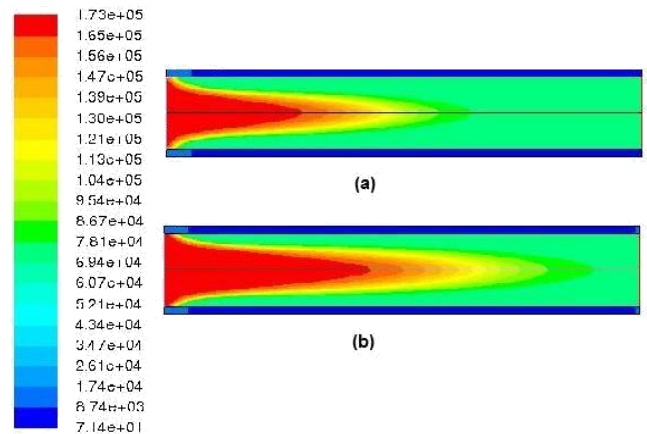
**5.2.2 Maximum Flame temperature:**

Fig 5.17 shows the maximum flame temperature comparison for methane and syngas for 2mm combustor having velocity 4 m/s, equivalence ratio 0.9 and robin’s boundary conditions at wall. As figure shows syngas flame temperature is 2500 k, which higher as compared to methane flame temperature.

**5.2.3 Effect of Inlet Velocity on Carbon mono oxide and carbon dioxide formation:**

Inlet velocity has been taken as uniform throughout for steady state flow. The main role of velocity in

reacting flows is to carry the motion of reaction zone and heat transfer between wall and mixture. Inlet velocity shifts the reaction zone towards the downstream direction. Also the velocity at inlet affects the flue gas concentration at axis. The highest concentration zone of CO also shifts at downstream direction. Taking all boundary conditions constant for stoichiometric ratio the velocities at inlet are subsequently changed and observed that inlet velocities decides the maximum



**Fig. 5.19: CO<sub>2</sub> concentration in 2mm combustor with syn gas at various velocities.**

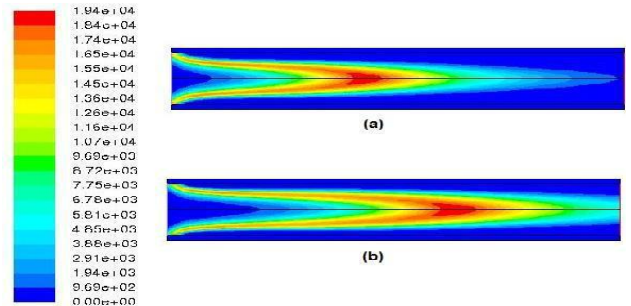


**Fig. 5.20: CO concentration in 2mm combustor with syn gas at various velocities.**

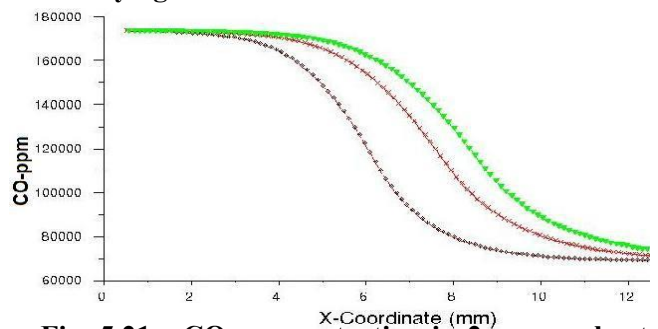


**Fig. 5.21: CO concentration in 2mm combustor of syn gas at various velocities at axis.**



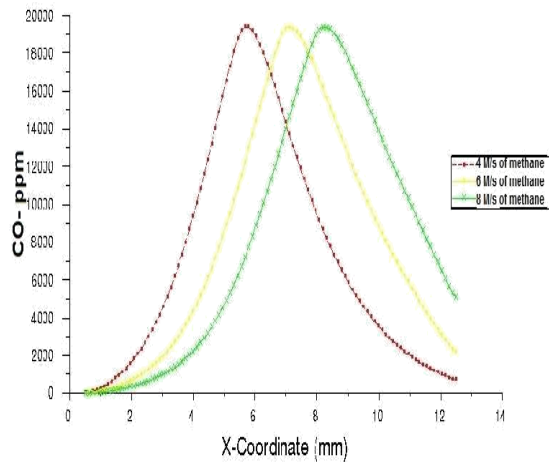


**Fig. 5.22: CO concentration in 2mm combustor of methane at various velocities at axis.**

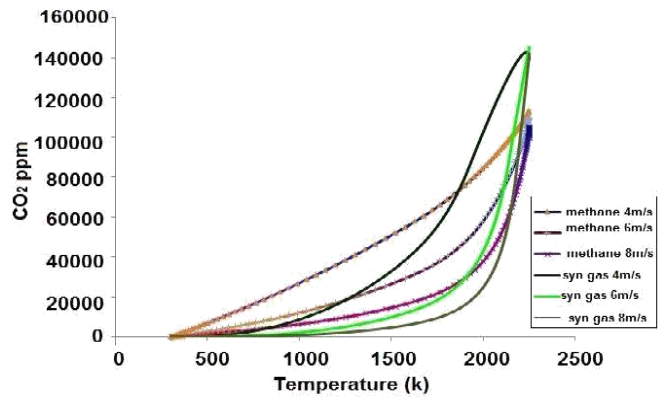


**Fig. 5.25: CO<sub>2</sub> mass fraction Vs Temperature at various velocities for methane.**

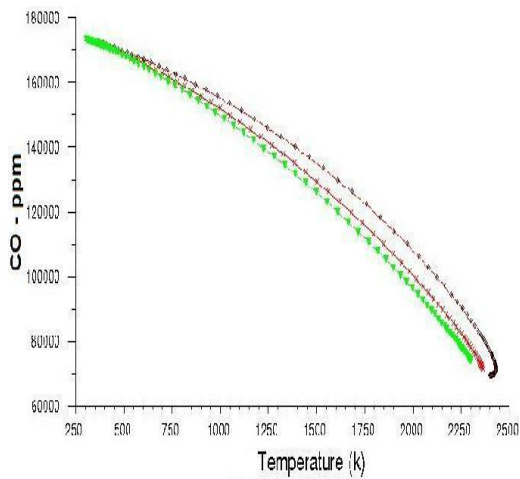


**Fig. 5.23: CO concentration of syn gas with combustor temperature at various velocities.**

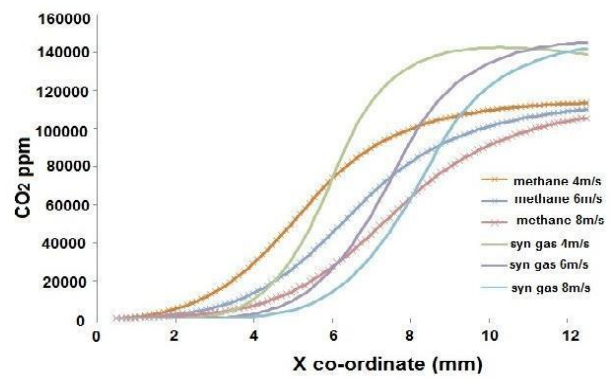


**Fig. 5.26: Comparison of CO<sub>2</sub> mass fraction at combustor axis for syngas and methane**

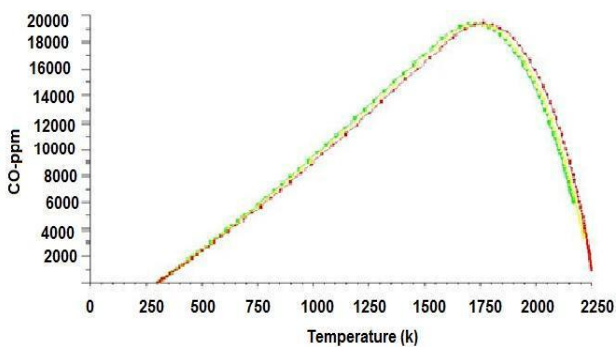


**Fig. 5.24: CO mass fraction Vs Temperature at various velocities for methane.**

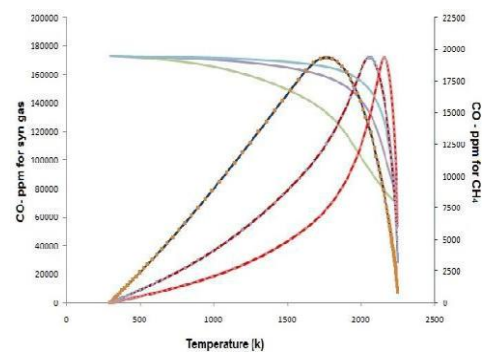


**Fig. 5.27: Comparison of CO mass fraction Vs Temperature for syngas and methane.**

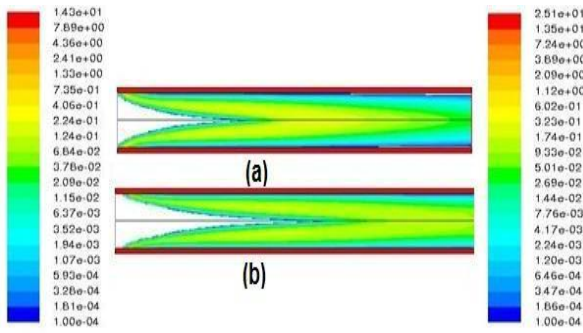


**Fig. 5.29: N<sub>2</sub>O concentration in combustor with different velocities for wall temperature profile**

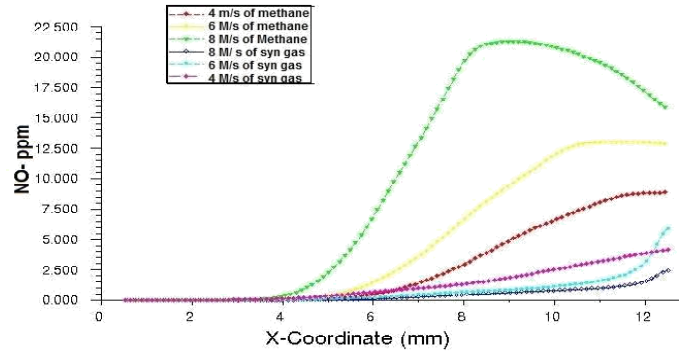


**Fig. 5.32: N<sub>2</sub>O ppm comparison for methane and syngas at combustor axis**

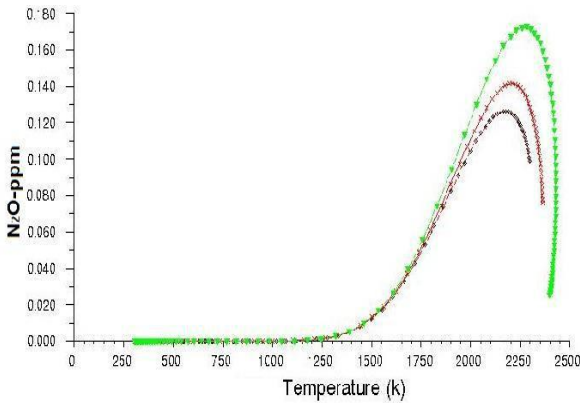


**Fig. 5.30 : N<sub>2</sub>O ppm for methane Vs combustor temperatures at axis.**

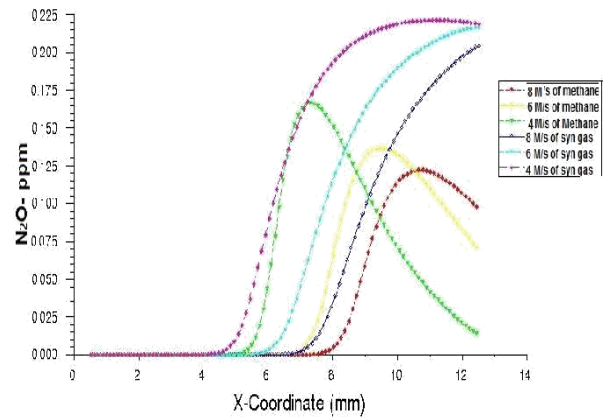


**Fig. 5.33: NO ppm comparison for syngas at combustor axis**

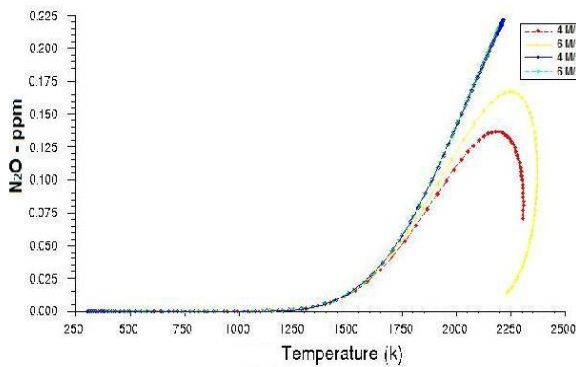


**Fig. 5.31 : N<sub>2</sub>O ppm for syngas Vs combustor temperatures at axis**

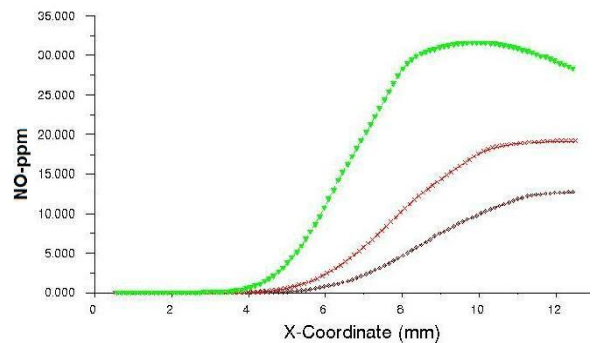


**Fig. 5.34 : NO ppm comparison for syngas and methane at combustor axis.**

## VI. Summary and Conclusion

### 6.1 For methane-air mixture:

The flame structure of premixed CH<sub>4</sub>-air in a small tube with a parabolic and constant velocity profiles at inlet for various equivalence ratios is numerically investigated. The effects of the inlet velocity, the equivalence ratio and the combustor size are discussed in this paper. From the above discussions, the main conclusions are summarized as follows:

1 The inlet velocity has a strong effect on combustion zone. The combustion zone shifts downstream as inlet velocity increases, however, temperature shows only slight variation.

2 The equivalence ratio is a key and dominating parameter that affects the combustion characteristics and hence the flame temperature. The highest flame temperature is obtained if the equivalence ratio is set at 0.9.

3 The combustor geometry is an important factor which affects the zone of maximum temperature in combustor. As in 1 mm diameter combustor the maximum temperature zone lies on axis because of smaller radius but in 2 mm diameter combustor more space is available in radial direction which promotes the radial diffusion over axial convection. Hence the spot of maximum temperature in 2 mm diameter combustor is shifted towards wall. As in small combustors the most difficult task is to maintain the steady and stable flame,

4 The wall temperature helps in maintaining the steady combustion which means the smaller combustor can be made with maintaining elevated wall temperatures and stable flames can be produced easily, also the temperature distribution along the flame can be proper which prevents the intense heat losses by the flames.

### 6.2 For syngas mixture:

The emission of CO in syn gas and CH<sub>4</sub>-air in a small tube for various inlet velocities an boundary condition is numerically investigated. The effects of the inlet velocity and Temperature are discussed in this paper.

From the above discussions, the main conclusions are summarized as follows:

1. The inlet velocity does not affect the maximum flame temperature but the Maximum CO concentration. The inlet velocity has strong influence on rate of formation and consumption of fuel. In case of carbon dioxide the inlet velocity strongly affects the emission and maximum concentration.
2. Maximum flame temperature is obtained with adiabatic walls and minimum CO emission is possible with lower velocities. And maximum temperature inside the combustor affects the emission norms.
3. In syn gas CO consumption rises with increase in combustor temperature while in methane CO concentration is maximum around outer envelope of flame it rises up to a certain temperature and decreases with further increase in temperature.
4. In syn gas and methane carbon dioxide concentration decreases with increase in velocity because of incomplete combustion.
5. For stoichiometric air-fuel ratios with same operating conditions syn gas emission of carbon mono oxide and carbon dioxide is more than methane-air mixture.

## VII. REFERENCES

- [1] Fernandez-Pello AC. Micropower generation using combustion: issues and approaches. Proceedings of the Combustion Institute 2002;29:883e99.
- [2] Niket S. Kaisare, Dionisios G. Vlachos A review on microcombustion: Fundamentals, devices and applications.
- [3] J.S. Hua, M. Wu, K. Kumar, Numerical simulation of the combustion of hydrogen-air mixture in micro-scaled chambers. Part II. CFD analysis for a micro-combustor, Chem. Eng. Sci. 60 (2005) 3507–3515.
- [4] X.C. Shan, Z.F. Wang, Y.F. Jin, M. Wu, J. Hua, C.K. Wong, R. Maeda, Studies on a micro combustor for gas turbine engines, J. Micromech. Microeng. 15 (2005) S215–221.

- [5] L. Sitzki, K. Borer, E. Schuster, P.D. Ronney, S.Wussow, Combustion in micro scale heat-recirculating burners, in: Proceedings of The Third Asia-Pacific Conference on Combustion, Seoul, Korea, 2001.
- [6] W.M. Yang, S.K. Chou, C. Shu, Z.W. Li, H. Xue, Development of micro thermophotovoltaic system, *Appl. Phys. Lett.* 81 (2002) 5255–5257.
- [7] W.M. Yang, S.K. Chou, C. Shu, H. Xue, Z.W. Li, Development of a prototype micro-thermophotovoltaic power generator, *J. Phys. D: Appl. Phys.* 37 (2004) 1017–1020.
- [8] A.C. Fernandez-Pello, Micropower generation using combustion: issues and approaches, *Proc. Combust. Inst.* 29 (2002) 883–898.
- [9] J. Li, S.K. Chou, W.M. Yang, Z.W. Li, A numerical study on premixed micro-combustion of CH<sub>4</sub>-air mixture: Effects of combustor size, geometry and boundary conditions on flame temperature. *Chemical Engineering Journal* 150 (2009) 213–222.
- [10] Liang Feng, Zhongliang Liu\*, Yanxia Li, Numerical study of methane and air combustion inside a small tube with an axial temperature gradient at the wall. *Chemical Engineering Journal* 150 (2009) 213–222.